



Design, synthesis, and evaluation of imidazo[1,2-*b*]pyridazine derivatives having a benzamide unit as novel VEGFR2 kinase inhibitors

Naoki Miyamoto, Yuya Oguro, Terufumi Takagi, Hidehisa Iwata, Hiroshi Miki, Akira Hori, Shinichi Imamura*

Pharmaceutical Research Division, Takeda Pharmaceutical Company Limited, 2-26-1, Muraokahigashi, Fujisawa, Kanagawa 251-8555, Japan

ARTICLE INFO

Article history:

Received 6 September 2012

Revised 4 October 2012

Accepted 5 October 2012

Available online 13 October 2012

Keywords:

VEGF

VEGFR2

Kinase inhibitor

Imidazo[1,2-*b*]pyridazine

ABSTRACT

The vascular endothelial growth factor (VEGF) signaling pathway has been implicated in tumor angiogenesis, and inhibition of the VEGF pathway is considered an efficacious method for treating cancer. Herein, we describe synthetic studies of imidazo[1,2-*b*]pyridazine derivatives as VEGF receptor 2 (VEGFR2) kinase inhibitors. The imidazo[1,2-*b*]pyridazine scaffold was designed and synthesized as a hinge binder according to the previously reported crystal structure of pyrrolo[3,2-*d*]pyrimidine **1** with VEGFR2. Structure–activity relationship studies revealed that *meta*-substituted 6-phenoxy-imidazo[1,2-*b*]pyridazine derivatives had potent affinity for VEGFR2. In particular, *N*-[3-(imidazo[1,2-*b*]pyridazin-6-yloxy)phenyl]-3-(trifluoromethyl)benzamide (**6b**) exhibited strong inhibitory activity against VEGFR2 with an IC₅₀ value of 7.1 nM, and it inhibited platelet-derived growth factor receptor β kinase with an IC₅₀ value of 15 nM.

© 2012 Elsevier Ltd. All rights reserved.

1. Introduction

Angiogenesis, which is the formation of new capillary blood vessels from preexisting ones, is a crucial process that promotes tumor growth, survival, and metastasis.¹ Since it was hypothesized that the inhibition of angiogenesis could be an effective strategy for cancer therapy in 1971,² several regulators of angiogenesis, such as vascular endothelial growth factor (VEGF), platelet-derived growth factor (PDGF), basic fibroblast growth factor (bFGF), and angiopoietin, have been identified.³ Among them, the VEGF signaling pathway that acts through the VEGF receptor 2 (VEGFR2, also known as KDR) has been shown to play a key role in the regulation of tumor angiogenesis, in which the binding of VEGF to VEGFR2 leads to receptor dimerization, which is followed by the autophosphorylation of tyrosine residues in the intracellular kinase domain, resulting in potent mitogenic and chemotactic effects on endothelial cells.^{4,5} The expression of VEGF is upregulated by tumor-related changes, such as hypoxia, protooncogene activation, and the aberration of tumor-suppressor genes.^{6–8} The overexpression of VEGF correlates with poor prognosis and the clinical stage of patients with solid tumors.^{9–11} Therefore, VEGF/VEGFR2 signaling has been thought to be an attractive target for the treatment of cancer. A humanized anti-VEGF monoclonal antibody (bevacizumab)¹² and small-molecule VEGFR2 kinase inhibitors (sorafenib,¹³ sunitinib,¹⁴ and pazopanib¹⁵) have been approved, and these have demon-

strated clinical benefits in the treatment of some tumors with manageable side effects. Many angiogenesis inhibitors are also being evaluated in clinical trials for the treatment of various cancers.¹⁶

In our previous study, we reported that the pyrrolo[3,2-*d*]pyrimidine derivative **1** (Fig. 1) had potent inhibitory activity against VEGFR2 kinase (IC₅₀ = 6.2 nM) and showed antitumor effects in a xenograft nude mouse model with human prostate cancer DU145 cells.¹⁷ The crystal structure analysis of compound **1** in complex with VEGFR2 revealed that **1** bound to the inactive form of VEGFR2 (Fig. 2). When **1** bound to VEGFR2, the N1-nitrogen of the pyrrolo[3,2-*d*]pyrimidine core formed a hydrogen bond with the backbone NH group of Cys919 in the hinge region. The urea NH and carbonyl groups interacted with Glu885 and Asp1046, respectively. The external phenyl group occupied a hydrophobic pocket that was created by the rearrangement of the protein. These observations were similar to those in the crystal structure of the known pyridine- and pyrimidine-based compounds that were bound with VEGFR2.¹⁸ Because the VEGFR2 kinase inhibitors possessing a fused or nonfused pyridine/pyrimidine core have been well investigated, our interest moved to new scaffolds for VEGFR2 kinase inhibitors, which are expected to acquire different kinase selectivities and novelties. Our strategy was the replacement of the pyrrolo[3,2-*d*]pyrimidine by other ring systems that have a hydrogen bond acceptor (HBA) nitrogen, so that the compounds retain the essential hydrogen bonding with the main chain of Cys919. Based on this strategy, we moved the HBA site from the 6-membered ring to the 5-membered ring, which resulted in the discovery of an imidazo[1,2-*b*]pyridazine core as a novel

* Corresponding author. Tel.: +81 466 32 1166; fax: +81 466 29 4448.

E-mail address: shin-ichi.imamura@takeda.com (S. Imamura).

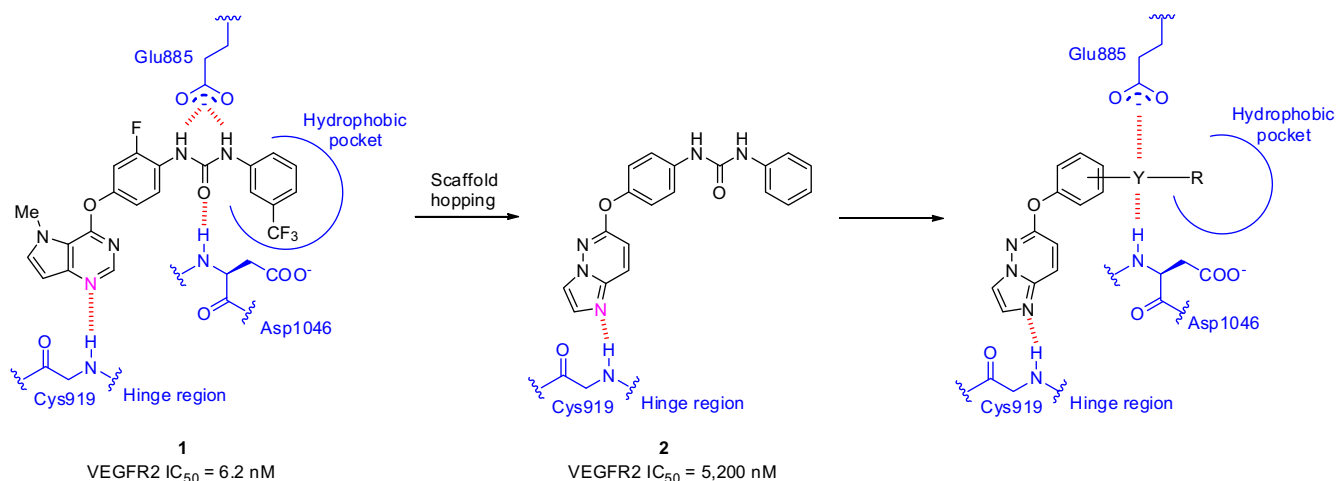


Figure 1. Design of imidazo[1,2-*b*]pyridazine derivatives.

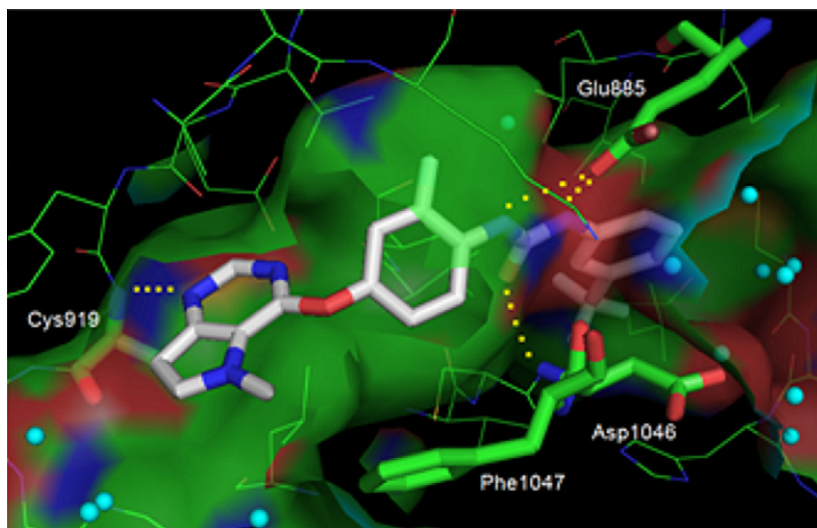


Figure 2. X-ray co-crystal structure of **1** in complex with VEGFR2 (PDB code 3VHE).¹⁷

hinge-binding template (**2**, Fig. 1). In fact, compound **2** showed moderate inhibitory activity against VEGFR2 kinase with an IC_{50} value of 5200 nM. Thus, we investigated phenoxy substituents (–Y–R) with the aim of finding more effective interactions with Glu885, Asp1046, and the hydrophobic pocket. In this paper, we describe the synthesis, structure–activity relationships, and characterization of these new inhibitors.

2. Chemistry

The target compounds were prepared according to the synthetic routes shown in Schemes 1 and 2. The 6-chloroimidazo[1,2-*b*]pyridazine (**3**)¹⁹ was treated with aminophenols in the presence of K_2CO_3 in order to obtain the 6-phenoxyimidazo[1,2-*b*]pyridazines **4a–c**, which were converted to the ureas **2** and **5a–d** with appropriate phenyl isocyanates (Scheme 1). The benzamides **6a** and **6b** were obtained by treatment of **4b** with benzoyl chloride and 3-(trifluoromethyl)benzoyl chloride, respectively.

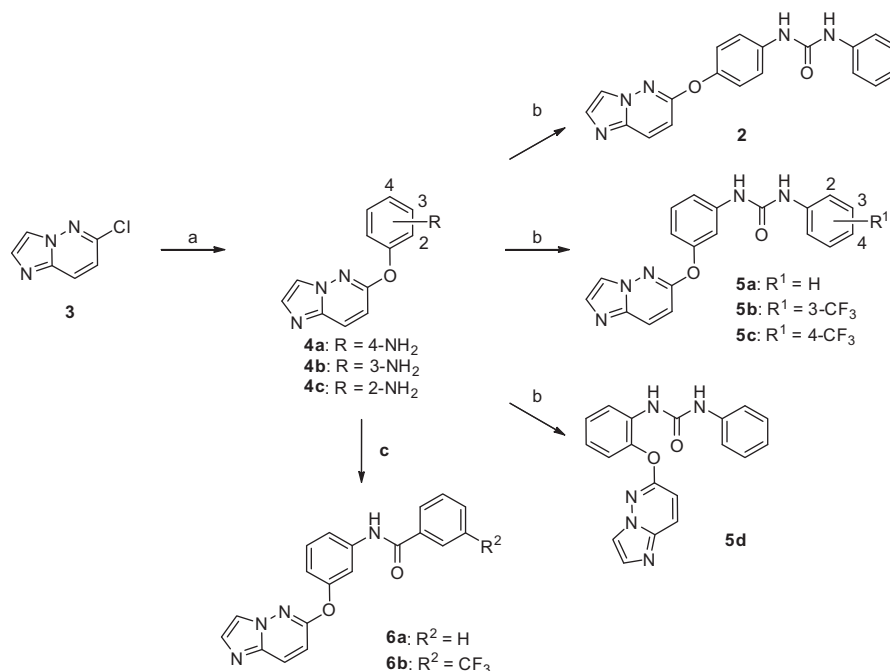
For the preparation of the amide analogs **8a** and **8b**, compound **3** was treated with methyl 3-hydroxybenzoate in the presence of K_2CO_3 to give the ester **7a** (Scheme 2). After the conversion of

the ester **7a** into the acid **7b** in basic conditions, **7b** was condensed with aniline and 3-(trifluoromethyl)aniline using 1-ethyl-3-[3-(dimethylamino)propyl]carbodiimide hydrochloride (EDC·HCl) and 1-hydroxybenzotriazole (HOBt) to provide the amides **8a** and **8b**, respectively.

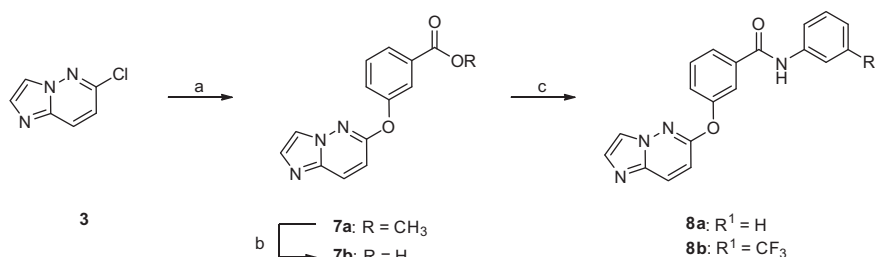
3. Results and discussion

The imidazo[1,2-*b*]pyridazine derivatives that are depicted in Tables 1 and 2 were evaluated for their inhibitory activities against human VEGFR2 kinase with a non-RI assay using the amplified luminescent proximity homogeneous assay (AlphaScreen) system.²⁰ AlphaScreen is based on the transfer of energy from donor to acceptor microbeads that are brought together by a biomolecular interaction. In this system, an anti-phosphotyrosine antibody is immobilized with the acceptor beads, and the biotinylated poly-GluTyr (4:1) is conjugated with streptavidin donor beads. The amount of phosphorylated substrate was measured from the signals of the AlphaScreen system.

In order to determine the best substitution position required for efficient interactions with Glu885/Asp1046 and the hydrophobic



Scheme 1. Reagents: (a) aminophenols, K₂CO₃, NMP; (b) phenyl isocyanates, Et₃N, THF; (c) benzoyl chlorides, NMP.

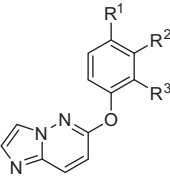


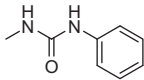
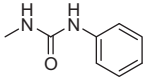
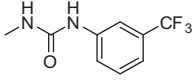
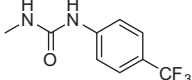
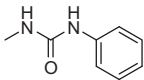
Scheme 2. Reagents: (a) methyl 3-hydroxybenzoate, K₂CO₃, NMP; (b) aq NaOH, MeOH; (c) anilines, HOBT, EDC·HCl, Et₃N, DMF.

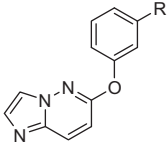
pocket of VEGFR2, we first prepared urea derivatives in which a phenylureido group was introduced at the *ortho*- and *meta*-positions of the phenoxy moiety (Table 1). Moving the phenylureido group of **2** from the *para*-position to the *meta*-position (**5a**) significantly increased the inhibitory activity against VEGFR2 kinase (**5a**: IC₅₀ = 52 nM), while the activity was diminished by placing it at the *ortho*-position (**5d**: IC₅₀ >10,000 nM). The imidazo[1,2-*b*]pyridazine derivatives preferred the *meta*-phenylureido group, although the pyrrolo[3,2-*d*]pyrimidine derivatives with the *para*-substituent were more potent than those with the *meta*-substituent.¹⁷ This difference between the imidazo[1,2-*b*]pyridazine and the pyrrolo[3,2-*d*]pyrimidine was probably derived from the difference in the HBA position that was interacting with the NH group of Cys919. Indeed, binding model analyses of compounds **2** and **5a** with VEGFR2 revealed that **5a** exhibited a reasonable binding mode, supporting its potent inhibitory activity (Fig. 3a) while an appropriate docking mode of **2** with VEGFR2 could not be obtained. The docking model of **5a** predicted the interaction between the N1-nitrogen of imidazo[1,2-*b*]pyridazine and the NH group of Cys919. In this model, the ureido group of **5a** formed hydrogen-bonding interactions with Glu885/Asp1046, and the terminal phenyl ring was located in the hydrophobic pocket. Moreover, there was an extra space that was available for the introduction of substituents around the terminal phenyl ring. This encouraged us to synthesize 3- and 4-(trifluoromethyl)phenyl urea derivatives **5b** and **5c**, because our previous research on the pyrrolo[3,2-*d*]pyrimidine derivatives

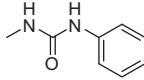
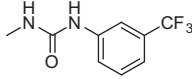
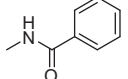
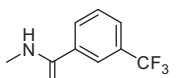
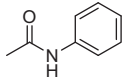
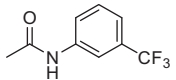
showed that incorporating a trifluoromethyl group was effective for filling the hydrophobic pocket.¹⁷ Both of them showed increased inhibitory activity against VEGFR2 compared to the non-substituted phenylurea **5a** (**5b**: IC₅₀ = 12 nM, **5c**: IC₅₀ = 29 nM). These activity gains were consistent with the results of the binding model analysis of **5b**, in which the 3-trifluoromethyl group fit into the hydrophobic pocket (Fig. 3b).

Thus, we concluded that a *meta*-substitution of the 6-phenoxy-imidazo[1,2-*b*]pyridazine scaffold was optimal for the inhibition of VEGFR2 kinase. We continued to pursue the best *meta*-substituents for interactions with VEGFR2 (Table 2). The amide derivatives **6a** and **8a** were designed to investigate the importance of the urea NH group in **5a**. Removal of the NH group that was attached to the terminal phenyl ring of **5a** (IC₅₀ = 52 nM) retained potency (**6a**: IC₅₀ = 80 nM), while removal of that attached to the central phenyl ring resulted in about a 10-fold loss of potency (**8a**: IC₅₀ = 640 nM). These results suggested that the amide proton of **6a** effectively contributed to the interaction with Glu885 as a hydrogen bond donor. In fact, the binding model of compound **6a** with VEGFR2 showed that the amide unit made hydrogen bonding interactions with Glu885/Asp1046 at an appropriate distance (Fig. 4). However, the inverse amide (**8a**) might lose the efficient interaction with Glu885/Asp1046 and/or the hydrophobic pocket due to its conformational change. Interestingly, potency increases were observed by the introduction of a trifluoromethyl group at the 3-position of the terminal phenyl ring (**6b**, **8b**). While the urea

Table 1
VEGFR2 kinase inhibitory activity of phenylurea derivatives


Compd	R ¹	R ²	R ³	VEGFR2 IC ₅₀ (nM) ^a
2				5200 (3500–7900)
5a				52 (34–81)
5b				12 (11–15)
5c				29 (19–42)
5d				>10,000

^a Numbers in parentheses represent 95% confidence interval.**Table 2**
VEGFR2 kinase inhibitory activity of *meta*-substituted 6-phenoxy-imidazo[1,2-*b*]pyridazines


Compd	R	VEGFR2 IC ₅₀ (nM) ^a
5a		52 (34–81)
5b		12 (11–15)
6a		80 (61–110)
6b		7.1 (6.0–8.2)
8a		640 (520–790)
8b		18 (11–29)

^a Numbers in parentheses represent 95% confidence interval.

5b was about fourfold more potent than **5a**, the amides **6b** and **8b** displayed more than 10-fold and 30-fold increases of activity compared to **6a** and **8a**, respectively (**6b**: IC₅₀ = 7.1 nM, **8b**:

IC₅₀ = 18 nM). One possible explanation for the differences in the fold changes is that the terminal phenyl rings of **6a** and **8a** occupied the hydrophobic pocket less efficiently than **5a** did. For **6b** and **8b**, the trifluoromethyl group might be appropriately located in the hydrophobic pocket, which significantly contributed to the increase of activity.

Compound **6b** was tested for its selectivity to 13 other kinases (Table 3). Compound **6b** showed strong inhibitory activity against VEGFR1, PDGF receptor α (PDGFR α), and PDGFR β with IC₅₀ values of 8.4, 13, and 15 nM, respectively. One of the reasons for the dual inhibition of the VEGFR and PDGFR kinases by **6b** is that the amino-acid sequence of the PDGFR kinase domain is similar to that of VEGFR (e.g. 73% similarity between PDGFR β and VEGFR2 kinase domains), and PDGFR kinase is on the same branch as VEGFR kinase in the human kinome tree.²¹ The PDGF/PDGFR pathway plays important roles in angiogenesis. The activation of PDGF/PDGFR signaling induces the proliferation and migration of pericytes, which lead to the formation of thicker and more stable blood vessels.^{22,23} Thus, the simultaneous inhibition of VEGFR and PDGFR kinases may enhance the efficacy of anti-angiogenic tumor therapy. On the other hand, the IC₅₀ values against the other kinases were over 4000 nM, except for the moderate inhibition against B-raf (IC₅₀ = 290 nM) and c-kit (IC₅₀ = 120 nM). Interestingly, **6b** displayed a much weaker inhibition against Tie-2 (IC₅₀ = 5100 nM) than pyrrolo[3,2-*d*]pyrimidine **1** (IC₅₀ = 20 nM). These results might be derived from the significant differences in their chemical structures. Thus, the imidazo[1,2-*b*]pyridazine derivative **6b** was found to be a selective inhibitor of VEGFR and PDGFR.

4. Conclusion

Utilizing the crystal structure information of the pyrrolo[3,2-*d*]pyrimidine **1** with VEGFR2, we designed and synthesized novel VEGFR2 inhibitors. Scaffold hopping from **1** resulted in the discovery of the imidazo[1,2-*b*]pyridazine derivative **2**, which showed moderate inhibitory activity against VEGFR2 kinase. Optimization

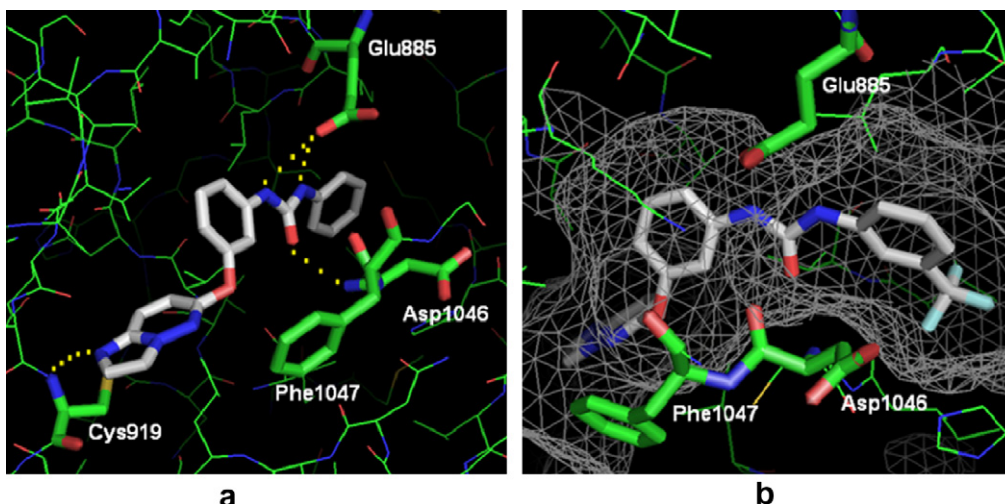


Figure 3. Binding model of imidazo[1,2-*b*]pyridazine derivatives and VEGFR2 using the crystal structure of **1** and VEGFR2. (a) Cartoon representation of the kinase with residues interacting with **5a**. (b) Surface representation of the back pocket region with **5b**.

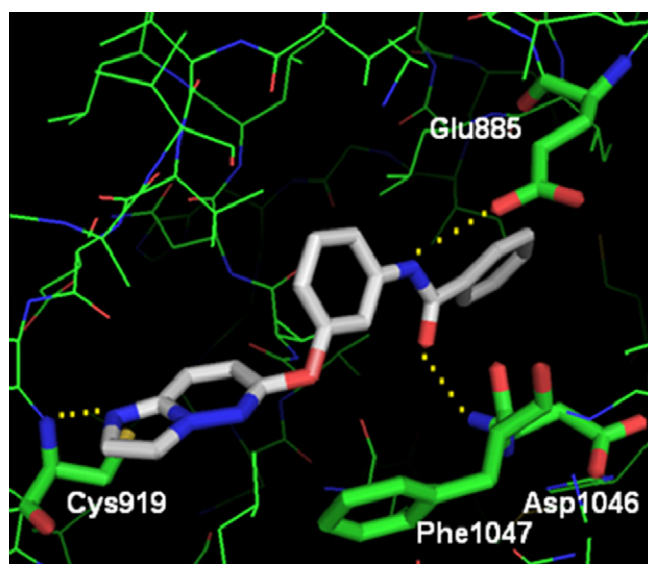


Figure 4. Binding model of the imidazo[1,2-*b*]pyridazine **6a** and VEGFR2.

of the phenylureido group of **2** revealed that *meta*-substitution was optimal, which led to the identification of **5a**. As a result of further

examination, the benzamide derivative **6a** was found to show similar potency to that of **5a**, and the introduction of a trifluoromethyl group at the 3-position of the external phenyl ring in **6a** led to the nanomolar VEGFR2 kinase inhibitor **6b**. Compound **6b** inhibited PDGFR kinase, as well as VEGFR kinase, and showed high selectivity over other kinases, such as Tie-2. Further optimization efforts in this series to find more efficacious angiogenesis inhibitors will be reported in the near future.

5. Experimental section

Commercial reagents and solvents were used without additional purification. Reaction progress was determined by thin layer chromatography (TLC) on Silica Gel 60 F254 plates (Merck) or NH TLC plates (Fuji Silysia). Column chromatography was carried out using a Purif Purification System (Moritex) with silica gel (Purif-Pack SI-60, Fuji Silysia) or basic silica gel (Purif-Pack NH-60, Fuji Silysia) cartridges. Melting points were determined on a Yanagimoto micro melting point, BÜCHI Melting Point B-545, or OptiMelt melting point apparatus and were not corrected. Proton nuclear magnetic resonance (^1H NMR) spectra were recorded on a Bruker DPX 300 (300 MHz) instrument. Chemical shifts (δ) are reported in ppm relative to internal tetramethylsilane. Peak multiplicities are expressed as follows: s, singlet; d, doublet; t, triplet; q, quartet; dd, doublet of doublet; dt, doublet of triplet; td, triplet of doublet; ddd, doublet of doublet of doublet; m, multiplet; br s, broad

Table 3
Kinase selectivity of **1** and **6b**

	IC_{50} (nM) ^a						
	VEGFR1	VEGFR2	PDGFR α	PDGFR β	FGFR1	FGFR3	FGFR4
1	15 (14–17)	6.2 (4.7–8.3)	35 (27–43)	96 (76–120)	>10,000	NT ^b	NT ^b
6b	8.4 (7.9–8.9)	7.1 (6.0–8.2)	13 (12–15)	15 (13–17)	5100 (4100–6400)	4200 (3000–5800)	>10,000
	IC_{50} (nM) ^a						
	c-kit	B-raf	GSK3 β	c-Met	Tie-2	IR	IGF1-R
1	170 (120–240)	900 (660–1200)	>10,000	NT ^b	20 (17–23)	>10,000	>10,000
6b	120 (99–140)	290 (200–430)	>10,000	>10,000	5100 (3600–7200)	>10,000	>10,000

^a Numbers in parentheses represent 95% confidence interval.

^b Not tested.

singlet. Coupling constants (*J*) are given in hertz (Hz). Elemental analyses were carried out at Takeda Analytical Research Laboratories, Ltd. Abbreviations are used as follows: DMF, *N,N*-dimethylformamide; DMSO, dimethyl sulfoxide; EDC-HCl, 1-ethyl-3-[3-(dimethylamino)propyl]carbodiimide hydrochloride; HOBt, 1-hydroxybenzotriazole; NMP, *N*-methylpyrrolidone; THF, tetrahydrofuran.

5.1. 4-(Imidazo[1,2-*b*]pyridazin-6-yloxy)aniline (**4a**)

A mixture of 6-chloroimidazo[1,2-*b*]pyridazine (**3**)¹⁹ (768 mg, 5.0 mmol), 4-aminophenol (818 mg, 7.5 mmol), and K₂CO₃ (2073 mg, 15.0 mmol) in NMP (5 mL) was stirred at 120 °C for 18 h. The mixture was diluted with 1 N aqueous NaOH and extracted with EtOAc. The organic layer was washed with 1 N aqueous NaOH and brine and concentrated in vacuo. The residue was purified by basic silica gel column chromatography (hexane/EtOAc 70:30 to 0:100) and triturated with diisopropyl ether to give **4a** (759 mg, 67%) as a gray solid. ¹H NMR (DMSO-*d*₆) δ 5.07 (2H, s), 6.60 (2H, d, *J* = 8.9 Hz), 6.92 (2H, d, *J* = 8.9 Hz), 7.00 (1H, d, *J* = 9.8 Hz), 7.61 (1H, s), 8.01 (1H, s), 8.09 (1H, d, *J* = 9.8 Hz).

5.2. 3-(Imidazo[1,2-*b*]pyridazin-6-yloxy)aniline (**4b**)

Compound **4b** was prepared from 3-aminophenol in a similar manner to that described for **4a**. Yield 41%, white solid. ¹H NMR (DMSO-*d*₆) δ 5.29 (2H, s), 6.31–6.35 (1H, m), 6.37 (1H, t, *J* = 2.2 Hz), 6.42–6.47 (1H, m), 7.02 (1H, d, *J* = 9.8 Hz), 7.06 (1H, t, *J* = 7.9 Hz), 7.65 (1H, d, *J* = 1.2 Hz), 8.08 (1H, s), 8.13 (1H, d, *J* = 9.8 Hz).

5.3. 2-(Imidazo[1,2-*b*]pyridazin-6-yloxy)aniline (**4c**)

Compound **4c** was prepared from 2-aminophenol in a similar manner to that described for **4a**. Yield 14%, pale brown solid. ¹H NMR (DMSO-*d*₆) δ 5.08 (2H, s), 6.57 (1H, td, *J* = 7.6, 1.6 Hz), 6.81 (1H, dd, *J* = 7.9, 1.7 Hz), 6.95–7.04 (2H, m), 7.04 (1H, d, *J* = 9.9 Hz), 7.61 (1H, d, *J* = 0.9 Hz), 8.02 (1H, s), 8.11 (1H, d, *J* = 9.9 Hz).

5.4. *N*-[4-(Imidazo[1,2-*b*]pyridazin-6-yloxy)phenyl]-*N'*-phenylurea (**2**)

To a solution of **4a** (181 mg, 0.80 mmol) and Et₃N (0.011 mL, 0.08 mmol) in THF (10 mL) was added phenyl isocyanate (0.104 mL, 0.96 mmol), and the mixture was stirred at room temperature for 18 h. The mixture was concentrated in vacuo. The residue was purified by basic silica gel column chromatography (EtOAc/MeOH 100:0 to 90:10) and triturated with EtOAc to give **2** (223 mg, 81%) as a white solid. Mp 197–199 °C. ¹H NMR (DMSO-*d*₆) δ 6.97 (1H, t, *J* = 7.6 Hz), 7.09 (1H, d, *J* = 9.8 Hz), 7.22 (2H, d, *J* = 8.7 Hz), 7.28 (2H, t, *J* = 7.6 Hz), 7.46 (2H, d, *J* = 7.6 Hz), 7.52 (2H, d, *J* = 8.7 Hz), 7.64 (1H, s), 8.05 (1H, s), 8.15 (1H, d, *J* = 9.8 Hz), 8.70 (1H, s), 8.76 (1H, s). Anal. Calcd for C₁₉H₁₅N₅O₂: C, 66.08; H, 4.38; N, 20.28. Found: C, 66.05; H, 4.34; N, 20.25.

5.5. *N*-[3-(Imidazo[1,2-*b*]pyridazin-6-yloxy)phenyl]-*N'*-phenylurea (**5a**)

Compound **5a** was prepared from **4b** and phenyl isocyanate in a similar manner to that described for **2**. Yield 71%, white solid. Mp 199–201 °C. ¹H NMR (DMSO-*d*₆) δ 6.85–6.90 (1H, m), 6.97 (1H, t, *J* = 7.5 Hz), 7.11 (1H, d, *J* = 9.6 Hz), 7.22–7.31 (3H, m), 7.36 (1H, t, *J* = 7.9 Hz), 7.43 (2H, d, *J* = 7.5 Hz), 7.51 (1H, t, *J* = 2.1 Hz), 7.66 (1H, d, *J* = 0.9 Hz), 8.08 (1H, s), 8.18 (1H, d, *J* = 9.6 Hz), 8.72 (1H, s), 8.87 (1H, s). Anal. Calcd for C₁₉H₁₅N₅O₂: C, 66.08; H, 4.38; N, 20.28. Found: C, 66.05; H, 4.38; N, 20.21.

5.6. *N*-[3-(Imidazo[1,2-*b*]pyridazin-6-yloxy)phenyl]-*N'*-[3-(trifluoromethyl)phenyl]urea (**5b**)

Compound **5b** was prepared from **4b** and 3-(trifluoromethyl)phenyl isocyanate in a similar manner to that described for **2**. Yield 62%, white solid. Mp 217–219 °C. ¹H NMR (DMSO-*d*₆) δ 6.89–6.94 (1H, m), 7.12 (1H, d, *J* = 9.8 Hz), 7.26–7.34 (2H, m), 7.38 (1H, t, *J* = 8.1 Hz), 7.47–7.60 (3H, m), 7.66 (1H, d, *J* = 0.9 Hz), 7.99 (1H, s), 8.08 (1H, s), 8.18 (1H, d, *J* = 9.8 Hz), 9.01 (1H, s), 9.11 (1H, s). Anal. Calcd for C₂₀H₁₄F₃N₅O₂: C, 58.11; H, 3.41; N, 16.94. Found: C, 58.05; H, 3.40; N, 16.83.

5.7. *N*-[3-(Imidazo[1,2-*b*]pyridazin-6-yloxy)phenyl]-*N'*-[4-(trifluoromethyl)phenyl]urea (**5c**)

Compound **5c** was prepared from **4b** and 4-(trifluoromethyl)phenyl isocyanate in a similar manner to that described for **2**. Yield 50%, white solid. Mp 246–247 °C. ¹H NMR (DMSO-*d*₆) δ 6.86–6.94 (1H, m), 7.11 (1H, d, *J* = 9.8 Hz), 7.24–7.31 (1H, m), 7.38 (1H, t, *J* = 8.2 Hz), 7.51 (1H, t, *J* = 1.8 Hz), 7.58–7.68 (5H, m), 8.08 (1H, s), 8.18 (1H, d, *J* = 9.8 Hz), 9.00 (1H, s), 9.16 (1H, s). Anal. Calcd for C₂₀H₁₄F₃N₅O₂: C, 58.11; H, 3.41; N, 16.94. Found: C, 57.95; H, 3.41; N, 16.76.

5.8. *N*-[2-(Imidazo[1,2-*b*]pyridazin-6-yloxy)phenyl]-*N'*-phenylurea (**5d**)

Compound **5d** was prepared from **4c** and phenyl isocyanate in a similar manner to that described for **2**. Yield 72%, white solid. Mp 213–214 °C. ¹H NMR (DMSO-*d*₆) δ 6.92–7.00 (1H, m), 7.02–7.09 (1H, m), 7.17–7.30 (5H, m), 7.38–7.44 (2H, m), 7.66 (1H, d, *J* = 0.9 Hz), 8.09 (1H, s), 8.20–8.28 (2H, m), 8.33 (1H, s), 9.04 (1H, s). Anal. Calcd for C₁₉H₁₅N₅O₂: C, 66.08; H, 4.38; N, 20.28. Found: C, 66.06; H, 4.33; N, 20.25.

5.9. *N*-[3-(Imidazo[1,2-*b*]pyridazin-6-yloxy)phenyl]benzamide (**6a**)

To a solution of **4b** (113 mg, 0.50 mmol) in NMP (1 mL) was added benzoyl chloride (0.116 mL, 1.0 mmol), and the mixture was stirred at room temperature for 18 h. The mixture was diluted with 1 N aqueous NaOH and extracted with EtOAc. The organic layer was washed with 1 N aqueous NaOH and brine and concentrated in vacuo. The residue was purified by silica gel column chromatography (EtOAc/MeOH 100:0 to 75:25) and recrystallized from EtOAc to give **6a** (122 mg, 74%) as a white solid. Mp 211–213 °C. ¹H NMR (DMSO-*d*₆) δ 7.01–7.06 (1H, m), 7.14 (1H, d, *J* = 9.8 Hz), 7.45 (1H, t, *J* = 8.2 Hz), 7.50–7.64 (3H, m), 7.66–7.71 (2H, m), 7.77 (1H, t, *J* = 2.1 Hz), 7.92–7.97 (2H, m), 8.09 (1H, s), 8.19 (1H, d, *J* = 9.8 Hz), 10.39 (1H, s). Anal. Calcd for C₁₉H₁₄N₄O₂: C, 69.08; H, 4.27; N, 16.96. Found: C, 68.99; H, 4.16; N, 16.72.

5.10. *N*-[3-(Imidazo[1,2-*b*]pyridazin-6-yloxy)phenyl]-3-(trifluoromethyl)benzamide (**6b**)

Compound **6b** was prepared from **4b** and 3-(trifluoromethyl)benzoyl chloride in a similar manner to that described for **6a**. Yield 98%, white solid. Mp 225–226 °C. ¹H NMR (DMSO-*d*₆) δ 7.05–7.10 (1H, m), 7.15 (1H, d, *J* = 9.6 Hz), 7.47 (1H, t, *J* = 7.9 Hz), 7.67–7.71 (1H, m), 7.67 (1H, d, *J* = 1.2 Hz), 7.75 (1H, t, *J* = 2.1 Hz), 7.79 (1H, t, *J* = 7.8 Hz), 7.98 (1H, d, *J* = 7.8 Hz), 8.09 (1H, s), 8.20 (1H, d, *J* = 9.6 Hz), 8.26 (1H, d, *J* = 8.4 Hz), 8.29 (1H, s), 10.61 (1H, s). Anal. Calcd for C₂₀H₁₃F₃N₄O₂·0.2EtOAc: C, 60.06; H, 3.54; N, 13.47. Found: C, 60.04; H, 3.59; N, 13.36.

5.11. Methyl 3-(imidazo[1,2-*b*]pyridazin-6-yloxy)benzoate (**7a**)

A mixture of **3** (1.54 g, 10 mmol), methyl 3-hydroxybenzoate (1.98 g, 13 mmol), and K_2CO_3 (4.15 g, 30 mmol) in NMP (10 mL) was stirred at 120 °C for 18 h. The mixture was diluted with water and extracted with EtOAc. The organic layer was washed with water and concentrated in vacuo. The residue was purified by basic silica gel column chromatography (hexane/EtOAc 90:10 to 20:80), silica gel column chromatography (hexane/EtOAc 60:40 to 0:100), and trituration with diisopropyl ether to give **7a** (1.72 g, 64%) as a white solid. 1H NMR (DMSO- d_6) δ 3.87 (3H, s), 7.16 (1H, d, J = 9.5 Hz), 7.60–7.68 (3H, m), 7.79–7.83 (1H, m), 7.84–7.93 (1H, m), 8.05 (1H, s), 8.19 (1H, d, J = 9.5 Hz).

5.12. 3-(Imidazo[1,2-*b*]pyridazin-6-yloxy)benzoic acid (**7b**)

To a solution of **7a** (1.67 g, 6.2 mmol) in MeOH (30 mL) was added 8 N aqueous NaOH (3.00 mL), and the mixture was stirred at room temperature for 18 h and at 80 °C for 8 h. After cooling to room temperature, the mixture was treated with 6 N HCl (4.00 mL) and concentrated in vacuo. The residue was suspended in water, and the precipitate was collected by filtration and washed with water. The precipitate was suspended in MeOH (10 mL), and the mixture was stirred at reflux for 10 min. After cooling to room temperature, the precipitate was collected by filtration and washed with MeOH to give **7b** (1.05 g, 66%) as a white solid. 1H NMR (DMSO- d_6) δ 7.15 (1H, d, J = 9.9 Hz), 7.54–7.68 (3H, m), 7.74–7.80 (1H, m), 7.82–7.91 (1H, m), 8.06 (1H, s), 8.19 (1H, d, J = 9.9 Hz), 13.17 (1H, br s).

5.13. 3-(Imidazo[1,2-*b*]pyridazin-6-yloxy)-*N*-phenylbenzamide (**8a**)

To a mixture of **7b** (128 mg, 0.50 mmol), aniline (56 mg, 0.60 mmol), and HOBt hydrate (92 mg, 0.60 mmol) in DMF (5 mL) were added EDC·HCl (192 mg, 1.0 mmol) and Et_3N (0.209 mL, 1.5 mmol), and the mixture was stirred at room temperature for 18 h. The mixture was diluted with 1 N aqueous NaOH and extracted with EtOAc. The organic layer was washed with water and brine and concentrated in vacuo. The residue was purified by silica gel column chromatography (EtOAc/MeOH 100:0 to 75:25) and trituration with EtOAc to give **8a** (122 mg, 74%) as a white solid. Mp 188–189 °C. 1H NMR (DMSO- d_6) δ 7.11 (1H, t, J = 7.4 Hz), 7.18 (1H, d, J = 9.6 Hz), 7.35 (2H, t, J = 7.9 Hz), 7.52–7.58 (1H, m), 7.63 (1H, d, J = 8.1 Hz), 7.66 (1H, d, J = 0.9 Hz), 7.73–7.80 (2H, m), 7.86–7.93 (2H, m), 8.07 (1H, s), 8.21 (1H, d, J = 9.6 Hz), 10.28 (1H, s). Anal. Calcd for $C_{19}H_{14}N_4O_2$: C, 69.08; H, 4.27; N, 16.96. Found: C, 69.12; H, 4.26; N, 16.95.

5.14. 3-(Imidazo[1,2-*b*]pyridazin-6-yloxy)-*N*-[3-(trifluoromethyl)phenyl]benzamide (**8b**)

Compound **8b** was prepared from **7b** and 3-(trifluoromethyl)aniline in a similar manner to that described for **8a**. Yield 57%, white solid. Mp 229–230 °C. 1H NMR (DMSO- d_6) δ 7.18 (1H, d, J = 9.9 Hz), 7.47 (1H, d, J = 7.8 Hz), 7.55–7.71 (4H, m), 7.89–7.95 (2H, m), 8.02–8.08 (2H, m), 8.19–8.25 (2H, m), 10.59 (1H, s). Anal. Calcd for $C_{20}H_{13}F_3N_4O_2$: C, 60.30; H, 3.29; N, 14.07. Found: C, 60.22; H, 3.25; N, 13.99.

5.15. Docking model of VEGFR2

The coordinate of the crystal structure of compound **1** with VEGFR2 was retrieved from the Protein Data Bank (accession code 3VHE). All imidazo[1,2-*b*]pyridazine derivatives were docked into the ligand binding pocket of VEGFR2, which was prepared by the removal of compound **1** from original coordinate, using GOLD

(version 3.0, the Cambridge Crystallographic Data Centre, UK) with the standard default settings. The initial docking models with VEGFR2 were energy-minimized using the MMFF94s force field in MOE (version 2005.06, Chemical Computing Group, Montreal, Canada) to obtain the final docking models. During the minimization procedure, the following conditions were adopted. The dielectric constant was set to $4 \times r$, where r is the interatomic distance. The residues, which are 8 Å away from compound, were fixed. The backbone atoms of protein were tethered to their initial positions with 10 kcal/Å² as a force constant. Atomic charges for the protein and the compounds were set according to the AMBER99 and the AM1-BCC method, respectively.

5.16. VEGFR2 kinase inhibition assay

The kinase activity of VEGFR2 was measured by use of an anti-phosphotyrosine antibody with the AlphaScreen® system (PerkinElmer, USA). Enzyme reactions were performed in 50 mM Tris-HCl pH 7.5, 5 mM $MnCl_2$, 5 mM $MgCl_2$, 0.01% Tween-20 and 2 mM DTT, containing 10 μ M ATP, 0.1 μ g/mL biotinylated poly-GluTyr(4:1) and 0.1 nM of VEGFR2 (Millipore, UK). Prior to catalytic initiation with ATP, compound and enzyme were incubated for 5 min at room temperature. The reactions were quenched by the addition of 25 μ L of 100 mM EDTA, 10 μ g/mL AlphaScreen streptavidine donor beads and 10 μ g/mL acceptor beads in 62.5 mM HEPES pH 7.4, 250 mM NaCl, and 0.1% BSA. Plates were incubated in the dark overnight and then read by EnVision 2102 Multilabel Reader (PerkinElmer, USA). Wells containing the substrate and the enzyme without compound were used as total reaction control. Wells containing biotinylated poly-GluTyr (4:1) and enzyme without ATP were used as basal control. The concentration of inhibitor producing 50% inhibition of the kinase activities (IC_{50} values) and 95% confidence intervals (95% CI) were analyzed using GraphPad Prism version 5.01, GraphPad Software (USA). Sigmoidal dose-response (variable slope) curves were fitted using non-linear regression analysis, with the top and bottom of the curve constrained at 100 and 0, respectively.

5.17. Kinase selectivity profiling

Kinase profiling was performed as described previously.^{17,24} Briefly, kinase activities of VEGFR1, VEGFR2, PDGFR α , PDGFR β , FGFR1, FGFR3, c-kit, c-Met, Tie-2, insulin receptor (IR), and insulin-like growth factor 1 receptor (IGF1-R) were measured by use of the AlphaScreen® system. For FGFR4, kinase assay was performed with 2 ng/mL FGFR4 (Millipore) and 20 μ M ATP. The kinase activities of glycogen synthase kinase-3 β (GSK-3 β) and B-raf were measured by use of radio labeled [γ -³³P] ATP. IC_{50} values and 95% CI were analyzed as described above.

Acknowledgment

The authors thank Ms. T. Yoshida for in vitro assays and Dr. K. Kamiyama for helpful discussion.

Supplementary data

Supplementary data associated with this article can be found, in the online version, at <http://dx.doi.org/10.1016/j.bmc.2012.10.004>. These data include MOL files and InChIKeys of the most important compounds described in this article.

References and notes

1. Folkman, J.; Merler, E.; Abernathy, C.; Williams, G. *J. Exp. Med.* **1971**, *133*, 275.
2. Folkman, J.; Shing, Y. *J. Biol. Chem.* **1992**, *267*, 10931.

3. (a) Klagsbrun, M.; Moses, M. A. *Chem. Biol.* **1999**, *6*, R217; (b) Rifkin, D. B.; Moscatelli, D. J. *Cell Biol.* **1989**, *109*, 1; (c) Nicosia, R. F.; Nicosia, S. V.; Smith, M. *Am. J. Pathol.* **1994**, *145*, 1023; (d) Suri, C.; McClain, J.; Thurston, G.; McDonald, D. M.; Zhou, H.; Oldmixon, E. H.; Sato, T. N.; Yancopoulos, G. D. *Science* **1998**, *282*, 468.
4. Shibuya, M.; Claesson-Welsh, L. *Exp. Cell Res.* **2006**, *312*, 549.
5. (a) Dougher, M.; Terman, B. I. *Oncogene* **1999**, *18*, 1619; (b) Hubbard, S. R. *Prog. Biophys. Mol. Biol.* **1999**, *71*, 343; (c) Strawn, L. M.; Shawver, L. K. *Expert Opin. Invest. Drugs* **1998**, *7*, 553.
6. Shweiki, D.; Itin, A.; Soffer, D.; Keshet, E. *Nature* **1992**, *359*, 843.
7. Kawasaki, K.; Watabe, T.; Sase, H.; Hiroshima, M.; Koide, H.; Morishita, Y.; Yuki, K.; Sasaoka, T.; Suda, T.; Katsuki, M.; Miyazono, K.; Miyazawa, K. *J. Cell Biol.* **2008**, *181*, 131.
8. Zhang, L.; Yu, D.; Hu, M.; Xiong, S.; Lang, A.; Ellis, L. M.; Pollock, R. E. *Cancer Res.* **2000**, *60*, 3655.
9. Guetz, G. D.; Uzzan, B.; Nicolas, P.; Cucherat, M.; Morere, J. F.; Benamouzig, R.; Breau, J. L.; Perret, G. Y. *Br. J. Cancer* **2006**, *94*, 1823.
10. Yuan, A.; Yu, C. J.; Chen, W. J.; Lin, F. Y.; Kuo, S. H.; Luh, K. T.; Yang, P. C. *Int. J. Cancer* **2000**, *89*, 475.
11. Jacobsen, J.; Grankvist, K.; Rasmuson, T.; Bergh, A.; Landberg, G.; Ljungberg, B. *Br. J. Urol. Int.* **2004**, *93*, 297.
12. (a) Hurwitz, H.; Fehrenbacher, L.; Novotny, W.; Cartwright, T.; Hainsworth, J.; Heim, W.; Berlin, J.; Baron, A.; Griffing, S.; Holmgren, E.; Ferrara, N.; Fyfe, G.; Rogers, B.; Ross, R.; Kabbinavar, F. N. *Engl. J. Med.* **2004**, *350*, 2335; (b) Sandler, A.; Gray, R.; Perry, M. C.; Brahmer, J.; Schiller, J. H.; Dowlati, A.; Lilienbaum, R.; Johnson, D. H. N. *Engl. J. Med.* **2006**, *355*, 2542; (c) Miller, K.; Wang, M.; Gralow, J.; Dickler, M.; Cobleigh, M.; Perez, E. A.; Shenkier, T.; Cella, D.; Davidson, N. E. *N. Engl. J. Med.* **2007**, *357*, 2666.
13. Strumberg, D. *Drugs Today* **2005**, *41*, 773.
14. Motzer, R. J.; Michaelson, M. D.; Redman, B. G.; Hudes, G. R.; Wilding, G.; Figlin, R. A.; Ginsberg, M. S.; Kim, S. T.; Baum, C. M.; DePrimo, S. E.; Li, J. Z.; Bello, C. L.; Theuer, C. P.; George, D. J.; Rini, B. I. *J. Clin. Oncol.* **2006**, *24*, 16.
15. Harris, P. A.; Bolor, A.; Cheung, M.; Kumar, R.; Crosby, R. M.; Davis-Ward, R. G.; Epperly, A. H.; Hinkle, K. W.; Hunter, R. N. III; Johnson, J. H.; Knick, V. B.; Laudeman, C. P.; Luttrell, D. K.; Mook, R. A.; Nolte, R. T.; Rudolph, S. K.; Szewczyk, J. R.; Truesdale, A. T.; Veal, J. M.; Wang, L.; Stafford, J. A. *J. Med. Chem.* **2008**, *51*, 4632.
16. (a) Roth, G. J.; Heckel, A.; Colbatzky, F.; Handschuh, S.; Kley, J.; Lehmann-Lintz, T.; Lotz, R.; Tontsch-Grunt, U.; Walter, R.; Hilberg, F. *J. Med. Chem.* **2009**, *52*, 4466; (b) Renhowe, P. A.; Pecchi, S.; Shafer, C. M.; Machajewski, T. D.; Jazan, E. M.; Taylor, C.; Antonios-McCrea, W.; McBride, C. M.; Frazier, K.; Wiesmann, M.; Lapointe, G. R.; Feucht, P. H.; Warne, R. L.; Heise, C. C.; Menezes, D.; Aardalen, K.; Ye, H.; He, M.; Le, V.; Vora, J.; Jansen, J. M.; Wernette-Hammond, M. E.; Harris, A. L. *J. Med. Chem.* **2009**, *52*, 278; (c) Polverino, A.; Coxon, A.; Starnes, C.; Diaz, Z.; DeMelfi, T.; Wang, L.; Bready, J.; Estrada, J.; Cattley, R.; Kaufman, S.; Chen, D.; Gan, Y.; Kumar, G.; Meyer, J.; Neervannan, S.; Alva, G.; Talvenheimo, J.; Montestruque, S.; Tasker, A.; Patel, V.; Radinsky, R.; Kendall, R. *Cancer Res.* **2006**, *66*, 8715; (d) Nakamura, K.; Taguchi, E.; Miura, T.; Yamamoto, A.; Takahashi, K.; Bichat, F.; Guilbaud, N.; Hasegawa, K.; Kubo, K.; Fujiwara, Y.; Suzuki, R.; Kubo, K.; Shibuya, M.; Isae, T. *Cancer Res.* **2006**, *66*, 9134; (e) Albert, D. H.; Tapang, P.; Magoc, T. J.; Pease, L. J.; Reuter, D. R.; Wei, R. Q.; Li, J.; Guo, J.; Bousquet, P. F.; Ghoreishi-Haack, N. S.; Wang, B.; Bukofzer, G. T.; Wang, Y. C.; Stavropoulos, J. A.; Hartandi, K.; Niquette, A. L.; Soni, N.; Johnson, E. F.; McCall, J. O.; Bouska, J. J.; Luo, Y.; Donawho, C. K.; Dai, Y.; Marcotte, P. A.; Glaser, K. B.; Michaelides, M. R.; Davidsen, S. K. *Mol. Cancer Ther.* **2006**, *5*, 995.
17. Oguro, Y.; Miyamoto, N.; Okada, K.; Takagi, T.; Iwata, H.; Awazu, Y.; Miki, H.; Hori, A.; Kamiyama, K.; Imamura, S. *Bioorg. Med. Chem.* **2010**, *18*, 7260.
18. (a) Manley, P. W.; Bold, G.; Brügggen, J.; Fendrich, G.; Furet, P.; Mestan, J.; Schnell, C.; Stolz, B.; Meyer, T.; Meyhack, B.; Stark, W.; Strauss, A.; Wood, J. *Biochim. Biophys. Acta* **2004**, *1697*, 17; (b) Miyazaki, Y.; Matsunaga, S.; Tang, J.; Maeda, Y.; Nakano, M.; Philippe, R. J.; Shibahara, M.; Liu, W.; Sato, H.; Wang, L.; Nolte, R. T. *Bioorg. Med. Chem. Lett.* **2005**, *15*, 2203; (c) Potashman, M. H.; Bready, J.; Coxon, A.; DeMelfi, T. M., Jr.; DiPietro, L.; Doerr, N.; Elbaum, D.; Estrada, J.; Gallant, P.; Germain, J.; Gu, Y.; Harmange, J. C.; Kaufman, S. A.; Kendall, R.; Kim, J. L.; Kumar, G. N.; Long, A. M.; Neervannan, S.; Patel, V. F.; Polverino, A.; Rose, P.; Plas, S.; Whittington, D.; Zanon, R.; Zhao, H. *J. Med. Chem.* **2007**, *50*, 4351; (d) Harmange, J. C.; Weiss, M. M.; Germain, J.; Polverino, A. J.; Borg, G.; Bready, J.; Chen, D.; Choquette, D.; Coxon, A.; DeMelfi, T.; DiPietro, L.; Doerr, N.; Estrada, J.; Flynn, J.; Graceffa, R. F.; Harriman, S. P.; Kaufman, S.; La, D. S.; Long, A.; Martin, M. W.; Neervannan, S.; Patel, V. F.; Potashman, M.; Regal, K.; Roveto, P. M.; Schrag, M. L.; Starnes, C.; Tasker, A.; Teffera, Y.; Wang, L.; White, R. D.; Whittington, D. A.; Zanon, R. *J. Med. Chem.* **2008**, *51*, 1649; (e) Cee, V. J.; Cheng, A. C.; Romero, K.; Bellon, S.; Mohr, C.; Whittington, D. A.; Bak, A.; Bready, J.; Caenepeel, S.; Coxon, A.; Deak, H. L.; Fretland, J.; Gu, Y.; Hodous, B. L.; Huang, X.; Kim, J. L.; Lin, J.; Long, A. M.; Nguyen, H.; Olivieri, P. R.; Patel, V. F.; Wang, L.; Zhou, Y.; Hughes, P.; Geuns-Meyer, S. *Bioorg. Med. Chem. Lett.* **2009**, *19*, 424.
19. Byth, K. F.; Cooper, N.; Culshaw, J. D.; Heaton, D. W.; Oakes, S. E.; Minshull, C. A.; Norman, R. A.; Paupit, R. A.; Tucker, J. A.; Breed, J.; Pannifer, A.; Rowsell, S.; Stanway, J. J.; Valentine, A. L.; Thomas, A. P. *Bioorg. Med. Chem. Lett.* **2004**, *14*, 2249.
20. Ullman, E. F.; Kirakossian, H.; Singh, S.; Wu, Z. P.; Irvin, B. R.; Pease, J. S.; Switchenko, A. C.; Irvine, J. D.; Dafforn, A.; Skold, C. N.; Wagner, D. B. *Proc. Natl. Acad. Sci. U.S.A.* **1994**, *91*, 5426.
21. Manning, G.; Whyte, D. B.; Martinez, R.; Hunter, T.; Sudarsanam, S. *Science* **2002**, *298*, 1912.
22. Pietras, K.; Sjöblom, T.; Rubin, K.; Heldin, C. H.; Östman, A. *Cancer Cell* **2003**, *3*, 439.
23. Abramsson, A.; Lindblom, P.; Betsholtz, C. *J. Clin. Invest.* **2003**, *112*, 1142.
24. Saitoh, M.; Kunitomo, J.; Kimura, E.; Hayase, Y.; Kobayashi, H.; Uchiyama, N.; Kawamoto, T.; Tanaka, T.; Mol, C. D.; Dougan, D. R.; Textor, G. S.; Snell, G. P.; Itoh, F. *Bioorg. Med. Chem.* **2009**, *17*, 2017.